THE JOURNAL OF BIOLOGICAL CHEMISTRY VOL. 282, NO. 48, pp. 34977–34986, NOVEMBER 30, 2007

A Charge Reversal Differentiates (p)ppGpp Synthesis by Monofunctional and Bifunctional Rel Proteins*

Received for publication, June 12, 2007, and in revised form, September 19, 2007 Published, JBC Papers in Press, October 2, 2007, DOI 10.1074/jbc.M704828200

Mathew Sajish[‡1], **Divya Tiwari**[§2], **Dimple Rananaware**[§], **Vinay Kumar Nandicoori**[§3], **and Balaji Prakash**[‡4]

From the [‡]*Department of Biological Sciences and Bioengineering, Indian Institute of Technology, Kanpur, 208016 and the* [§]*National Institute of Immunology, Aruna Asaf Ali Marg, New Delhi 110067 India*

A major regulatory mechanism evolved by microorganisms to combat stress is the regulation mediated by (p)ppGpp (the stringent response molecule), synthesized and hydrolyzed by Rel proteins. These are divided into bifunctional and monofunctional proteins based on the presence or absence of the hydrolysis activity. Although these proteins require Mg^{2+} for (p)ppGpp synthesis, high Mg^{2+} was shown to inhibit this reaction in bifunctional Rel proteins from *Mycobacterium tuberculosis and Streptococcus equisimilis*. This is not a characteristic feature in enzymes that use a dual metal ion mechanism, such as DNA polymerases that are known to carry out a similar pyrophosphate transfer reaction. Comparison of polymerase Polβ and Rel_{Seq} structures that share a common fold led to the proposal that the latter would follow a single metal ion mechanism. Surprisingly, in contrast to bifunctional Rel, we did not find inhibition of guanosine 5′-triphosphate, 3′-diphosphate (pppGpp) synthesis at higher Mg^{2+} in the monofunctional RelA from *Escherichia coli*. We show that a charge reversal in a conserved motif in the synthesis domains explains this contrast; an R*X*KD motif in the bifunctional proteins is reversed to an E*X*DD motif. The differential response of these proteins to Mg^{2+} could also be noticed in fluorescent nucleotide binding and circular dichroism experiments. In mutants where the motifs were reversed, the differential effect could also be reversed. We infer that although a catalytic Mg^{2+} is common to both bifunctional and monofunctional proteins, the latter would utilize an additional metal binding site formed by E*X*DD. This work, for the first time, brings out differences in (p)ppGpp synthesis by the two classes of Rel proteins.

In the living world, prokaryotes are the most successful due to the way they respond to changes. They have evolved a plethora of cellular regulatory mechanisms to combat the adverse environmental conditions among which stringent response is most well characterized. The hallmark of stringent response is the accumulation of an effector molecule (p)ppGpp[5] (1–3). These molecules are responsible for the rapid shut down of stable RNA biosynthesis and up-regulation of specific genes involved in amino acid biosynthesis under stress conditions (4–6). Also, the importance of (p)ppGpp arises due to several roles that it plays in pathogenic bacteria such as *Mycobacterium tuberculosis* (7–13).

Synthesis and hydrolysis of (p)ppGpp are carried out by two distinct domains in the N-terminal region of the Rel family of proteins that are divided into a bifunctional class (that synthesizes and hydrolyzes) and a monofunctional class (that can only synthesize). This difference arises due to the absence of a well conserved HD*XX*ED motif required for (p)ppGpp hydrolysis in the latter. Although the N-terminal (~1–395) region of these proteins is sufficient to catalyze synthesis and hydrolysis reactions, the C-terminal domain ensures regulation of these antagonistic activities (14, 15). Given the critical role that Rel proteins play, it is important to understand the mechanism of (p)ppGpp metabolism.

The synthesizing domains of Rel proteins are classified along with enzymes that catalyze a pyrophosphate transfer reaction. Although most of these enzymes utilize a dual divalent cation mechanism, Rel has been proposed to follow a single-cation mechanism. This proposal was based on the following observations. (p)ppGpp synthesis by the bifunctional Rel proteins from *M. tuberculosis* (Rel_{Mtb}) and *Streptococcus equisimilis* (Rel_{Seq}) is inhibited when Mg^{2+} concentration is higher than that of NTPs, which is not the case for proteins employing a dual divalent cation mechanism (16–18). Besides this, Rel_{Seq} structure identified the palm domain of DNA polymerase (Polβ), also known to follow a dual cation mechanism (19) as the closest relative of the synthesis domain. Of the three conserved Asp residues that coordinate two Mg^{2+} ions in Polβ, only two carboxylic groups, namely Asp-264 and Glu-323, are conserved in Rel_{Seq}. These were implicated in coordinating the catalytic Mg^{2+} along with ATP in the active site (20). The observed inhibition of (p)ppGpp synthesis at high Mg^{2+}, the absence of a third conserved carboxylic residue, and the lack of electron density for Mg^{2+} in Rel_{Seq}, despite supplying it during crystalli-

* This work was supported in part by grants from Wellcome Trust, UK in the form of an International Senior Research Fellowship (to B. P.) and by the generous funding provided by Dept. of Biotechnology, India (to B. P. and V. K. N.) to the National Institute of Immunology. The costs of publication of this article were defrayed in part by the payment of page charges. This article must therefore be hereby marked "*advertisement*" in accordance with 18 U.S.C. Section 1734 solely to indicate this fact.

[1] The recipient of a National Doctoral Fellowship from the All India Council for Technical Education.
[2] A Senior Research Fellow of the Council of Scientific and Industrial Research, India.
[3] To whom correspondence may be addressed. Tel.: 91-11-26703789; Fax: 91-11-26742125; E-mail: vinaykn@nii.res.in.
[4] To whom correspondence may be addressed: Tel.: 91-512-2594013; Fax: 91-512-2594010; E-mail: bprakash@iitk.ac.in.

[5] The abbreviations used are: (p)ppGpp, general notation for both ppGpp and pppGpp; ppGpp, guanosine 5′-diphosphate,3′-diphosphate; pppGpp, guanosine 5′-triphosphate, 3′-diphosphate; Polβ, DNA polymerase; mant, *N*-methyl-3′-*O*-anthranoyl; WT, wild type; MT, mutant.

zation, led Hogg *et al.* (20) to propose a single-cation mechanism for Rel proteins.

Surprisingly, in contrast to the bifunctional Rel_{Mtb} and Rel_{Seq}, we did not find inhibition of pppGpp synthesis at higher Mg^{2+} by their monofunctional homologue in *Escherichia coli* ($RelA_{E.\ coli}$). We associate this contrast to a charge reversal in a conserved motif in the synthesizing domains of Rel proteins. An R*X*KD motif in the bifunctional proteins is substituted by an E*X*DD motif in the monofunctional proteins, which possibly forms a second metal binding site other than the one used by catalytic Mg^{2+}. The significance of these motifs in determining the differential effect of Mg^{2+} on (p)ppGpp synthesis is further substantiated by fluorescent nucleotide binding and circular dichroism (CD) experiments (21–23).

EXPERIMENTAL PROCEDURES

Cloning, Expression, and Purification—The bifunctional Rel_{Mtb} consists of 790 amino acids. PCR product corresponding to the N-terminal domain (amino acids 53–446) of *M. tuberculosis rel* was amplified using forward (5′-TTAGAATTCCATATGACCGCCCAACGCAGCACCACC-3′) and reverse (5′-GGATCCAAGCTTTTACCAGTCGAGCAGCTGACGCATCCA-3′) primers from *M. tuberculosis* genomic DNA using *Pfu* DNA polymerase (Stratagene). The amplicon was digested with NdeI and HindIII and cloned into corresponding sites in the pQE-2 expression vector (Qiagen). *E. coli RelA* consists of 744 residues, of which the N-terminal domain (1–395) was amplified from its genomic DNA using primers 5′-GTTGCGGCATATGGTTGCGGTAAGAAGTGC-3′ and 5′-AATAAGCTTTAAGCTGCGTACTTCGTCGAG-3′ and similarly cloned into pQE-2 vector.

Protein expression was carried out in *E. coli*. DH5α cells from 500 ml of growth medium were resuspended in 50 mM Tris-HCl (pH 8), 300 mM NaCl, 1 mM protease inhibitor mixture (Sigma), 1 mM dithiothreitol, 1% Triton X-100, and 5% glycerol. Cells were lysed by sonication. The supernatant, clarified by centrifugation at 35,000 relative centrifugal force for 30 min, was loaded onto a nickel-nitrilotriacetic acid column (Amersham Biosciences). The column was washed with 10 column volumes of wash buffer containing 20 mM Tris-HCl (pH 8.0), 500 mM NaCl, 1 mM dithiothreitol, and 25 mM imidazole. For eluting the protein, an imidazole gradient of 20 column volumes (0–0.5 M) was used, and the protein was eluted at 20% of the gradient. The purified protein was then subjected to gel filtration chromatography (Superdex 75, Amersham Biosciences). The buffer was exchanged with 50 mM HEPES, (pH 8), 200 mM NaCl, 1 mM dithiothreitol. The monomer fractions of the proteins were collected and stored at −80 °C after snap-freezing in liquid N_2. Here, the N-terminal halves of Rel proteins from *M. tuberculosis* (53–446) and *E. coli* (1–395) are referred to as Rel_{Mtb} and $RelA_{E.\ coli}$, respectively, unless mentioned otherwise.

pppGpp Synthesis Assays—pppGpp synthesis assays were carried out in a 5-μl reaction volume containing 0–50 mM HEPES (pH 8), 100 mM NaCl, 1 mM dithiothreitol, 10 mM $MgCl_2$, 1 mM GTP, 1 mM ATP, and 1 μCi of [γ-^{32}P]ATP and 5 μM Rel proteins at 37 °C for 30 min. The reaction was stopped by adding 1 μl of 6 M formic acid. The mixture was then centrifuged at 13,000 rpm for 10 min. 5 μl of the sample was spotted on the polyethyleneimine-coated TLC (Merck), resolved in 1.5 M KH_2PO_4 (pH 3.4) buffer, and subjected to autoradiography to detect the formation of pppGpp. Autoradiograms were aligned with the TLC plate, spots corresponding to pppGpp were cored out, and the counts (cpm) were determined using the scintillation counter. cpm obtained at 1 mM Mg^{2+} concentration was normalized to 100%. The percentage of activity for the other samples were calculated with respect to activity (cpm) at 1 mM Mg^{2+}.

Sequence Retrieval and Alignment—Protein sequences were obtained from SwissProt/Trembl (expasy.org/sprot/) and NCBI (www.ncbi.nlm.nih.gov/) databases. The protein sequences that belong to the Rel family were extracted and manually scanned for the presence of residues involved in (p)ppGpp synthesis and hydrolysis. An HD*XX*ED motif in the hydrolyzing domains coordinates a Mn^{2+} ion and participates in (p)ppGpp hydrolysis reaction (16). Therefore, the proteins were grouped into the bifunctional class when HD*XX*ED motif was present and into the monofunctional class if it was absent since the latter can only synthesize (p)ppGpp. Multiple sequence alignment of all the sequences was performed using ClustalX (24). Following this, careful manual examination ensured the alignment of conserved motifs.

Site-directed Mutagenesis—Site-directed mutagenesis was carried out by the overlapping PCR method. Forward and reverse primers were designed with the desired change in the codon sequence (underlined in the primer sequence). In Rel_{Mtb}, Arg-348 and Lys-350 were mutated to Glu and Asp, respectively. Primers used are as follows: Rel_{Mtb} R348E/K350D forward primer, 5′-GATGGCGGGTGAGTTCGACGACTACATCGC-3′; Rel_{Mtb} R348E/K350D reverse primer, 5′-GCGATGTAGTCGTCGAACTCACCCGCCATC-3′. In $RelA_{E.\ coli}$, Glu-306 and Asp-308 were mutated to Arg and Lys, respectively. Primers used are as follows: $Rel_{E.\ coli}$ E306R/D308K forward primer, 5′-CGCCACCTGCCCGGGCGGTTTAAGGATTACGTCGC-3′; $RelA_{E.\ coli}$ E306R/D308K reverse primer, 5′-GCGACGTAATCCTTAAACCGCCCGGGCAGGTGGCG-3′. In each case, the fragments were amplified using forward primer of the gene and the reverse primer containing the mutation and the reverse primer of the gene and the forward primer with the mutation. Amplicons were gel-purified, and equal quantities of both fragments were used as template for the second round of PCR amplification using forward and reverse primers originally used for amplifying the gene. The full-length amplicon for the mutant gene was digested with NdeI and HindIII and cloned into corresponding sites in pQE-2 vector.

mant-Nucleotide Binding Assays—Fluorescent nucleotide binding studies were carried out using LS 55 Fluorescence Spectrometer (PerkinElmer Life Sciences) at room temperature. The *N*-methyl-3′-*O*-anthranoyl (mant) group attached to the nucleotides was monitored with an excitation wavelength of 350 nm (slit width of 2.5 nm) and emission wavelength of 400–500 nm (slit width of 5 nm). Emission and excitation profiles of mant-nucleotides were generated from 0.2 μM free mant-GTP and mant-ATP in buffer. Protein mant-nucleotide complexes were generated by preincubating various concentrations of proteins (1–5 μM) with 0.2 μM mant-nucleotides in buffers supplemented with or without 1 mM EDTA for 10 min

at room temperature. The effect of Mg^{2+} on the interaction of Rel proteins with mant-GTP and mant-ATP was determined by comparing with 0.2 μM mant-GTP or mant-ATP fluorescence and 4 μM proteins in a buffer supplemented with 0–10 mM $MgCl_2$.

Circular Dichroism Experiments—CD spectra were recorded at 22 °C on a Jasco J-715 spectropolarimeter. A total of 1 μM of the proteins was used for CD studies. Protein samples were filtered through a 0.2-μm filter (Millipore) prior to use. Scans were taken at a bandwidth 1.5 nm, response time 2 s, data pitch 0.2 nm, and scanning speed of 50 nm/min from 250 to 200 nm in a quartz cuvette of path length 1 mm. Spectra were averaged over 10 scans.

RESULTS

pppGpp Synthesis by Monofunctional $RelA_{E.\ coli}$ Is Not Inhibited at Higher Mg^{2+} Concentrations—Rel proteins that are well characterized to synthesize and hydrolyze (p)ppGpp contain about 700–750 amino acids. Rigorous biochemical studies using Rel_{Mtb} and Rel_{Seq} have shown that the N-terminal (~1–395) region of these proteins is sufficient to catalyze these reactions efficiently (15, 18). Therefore, for the proteins mentioned in this study, Rel_{Mtb}, Rel_{Seq} and $RelA_{E.\ coli}$ indicate their N-terminal regions, whereas the full-length proteins are indicated explicitly, when required.

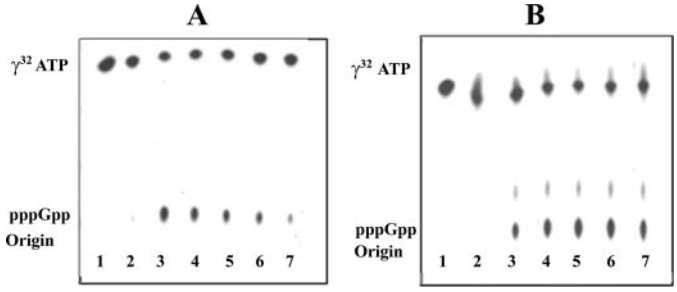

FIGURE 1. **pppGpp synthesis is inhibited as Mg^{2+} concentration is increased in Rel_{Mtb} (*A*), a bifunctional enzyme, but not in monofunctional $RelA_{E.\ coli}$ (*B*).** The reaction assayed was *pppA (ATP) + pppG (GTP) → pppGpp* + pA (AMP). * indicates the position of the radioactive label. A 5-μl reaction mixture was spotted on polyethyleneimine-TLC plates, separated, and visualized as described under "Experimental Procedures." The amount of pppGpp produced under varying $MgCl_2$ is shown from *lanes 1–7*. *Lane 1*, negative control with out the proteins; *lane 2*, 1 mM EDTA (0 mM $MgCl_2$); *lane 3*, 2 mM $MgCl_2$; *lane 4*, 5 mM $MgCl_2$; *lane 5*, 10 mM $MgCl_2$; *lane 6*, 25 mM $MgCl_2$; *lane 7*, 50 mM $MgCl_2$.

pppGpp Synthesis by Monofunctional $RelA_{E.\ coli}$ Is Not Inhibited at Higher Mg^{2+} Concentrations—Rel proteins that are well characterized to synthesize and hydrolyze (p)ppGpp contain about 700–750 amino acids. Rigorous biochemical studies using Rel_{Mtb} and Rel_{Seq} have shown that the N-terminal (~1–395) region of these proteins is sufficient to catalyze these reactions efficiently (15, 18). Therefore, for the proteins mentioned in this study, Rel_{Mtb}, Rel_{Seq} and $RelA_{E.\ coli}$ indicate their N-terminal regions, whereas the full-length proteins are indicated explicitly, when required.

A small excess of Mg^{2+}, above that of the substrate concentration, was reported to drastically reduce (p)ppGpp synthesis by the bifunctional enzymes Rel_{Mtb} (full-length) and Rel_{Seq} (17, 18). A complete inhibition of synthetase activity was observed for the former, whereas a residual activity was seen in the latter. This difference seems to be due to the use of full-length Rel_{Mtb} *versus* the N-terminal region (53–446) of Rel_{Seq} that was employed in the studies. Overall, Mg^{2+} seems to inhibit (p)ppGpp synthesis by bifunctional Rel proteins. We investigated whether Mg^{2+} can confer a similar effect on the synthesis activity by monofunctional $RelA_{E.\ coli}$. The reaction was ATP + GTP → pppGpp + AMP; pppGpp synthesis by both Rel_{Mtb} and $RelA_{E.\ coli}$ was measured (see "Experimental Procedures") at constant levels of enzyme and substrates while varying Mg^{2+} concentrations from 0 to 50 mM (25 times higher than ATP/GTP concentration). Fig. 1*A* shows that the amount of pppGpp synthesized by Rel_{Mtb} decreases significantly as the concentration of Mg^{2+} is increased. Here, unlike for Rel_{Mtb}(full-length), a residual activity is observed as in the case of Rel_{Seq} (18). In contrast, the amount of pppGpp synthesized by $RelA_{E.\ coli}$ was not affected under similar conditions (Fig. 1*B*, and see also Fig. 3*C*). This indicates a clear difference in metal requirement by $RelA_{E.\ coli}$ and Rel_{Mtb}, Rel_{Seq}, possibly suggesting differences in the reaction mechanism, despite a 59.3% sequence similarity in their synthesizing domains. The following studies were designed to further characterize this intriguing observation.

A Charge Reversal in a Conserved Motif Distinguishes the Bifunctional and Monofunctional Proteins—The differential response to Mg^{2+} by monofunctional $RelA_{E.\ coli}$ and bifunctional Rel_{Mtb}, Rel_{Seq} enzymes led us to inquire whether this is an attribute of all monofunctional and bifunctional proteins. To corroborate this, we resorted to analyzing the sequences of all Rel proteins (see "Experimental Procedures"). Although the sequence alignment displayed several conserved motifs across species, our attempt to search for motifs that distinguish the bifunctional and monofunctional proteins led to the identification of a unique charge reversal in a conserved motif in the (p)ppGpp synthesizing domains. An RXKD motif, conserved in all the bifunctional proteins, is substituted by an EXDD motif, conserved in all the monofunctional proteins (Fig. 2). An examination of the available structure of Rel_{Seq} (20) hinted at the

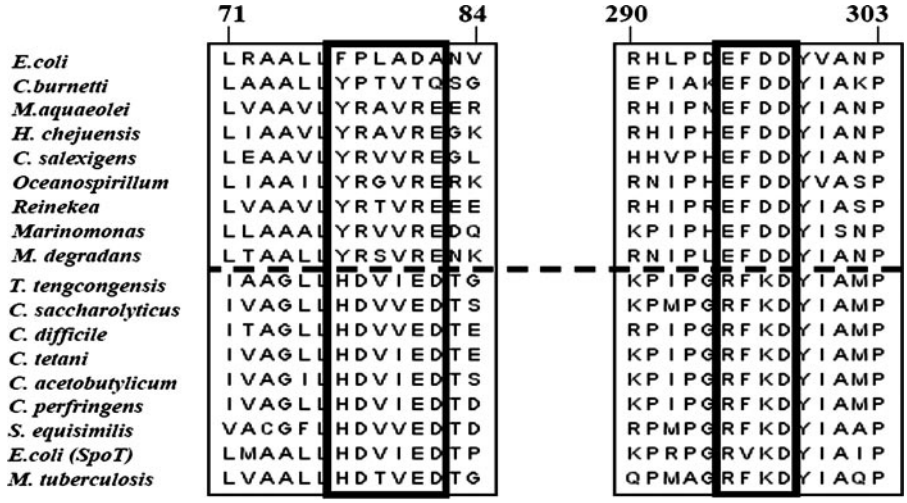

FIGURE 2. **A charge reversal in a conserved motif distinguishes monofunctional and bifunctional Rel proteins.** R*X*KD motif in bifunctional proteins is substituted by E*X*DD motif in monofunctional proteins (*boxed*). Bifunctional and monofunctional Rel proteins (separated by a dotted line) are grouped based on the presence or absence of HD*XX*ED motifs (*boxed*). Relevant regions (containing these motifs) of the multiple sequence alignment of sequences representing these two groups are shown. The *numbers* above the alignment correspond to those of Rel_{Seq}.

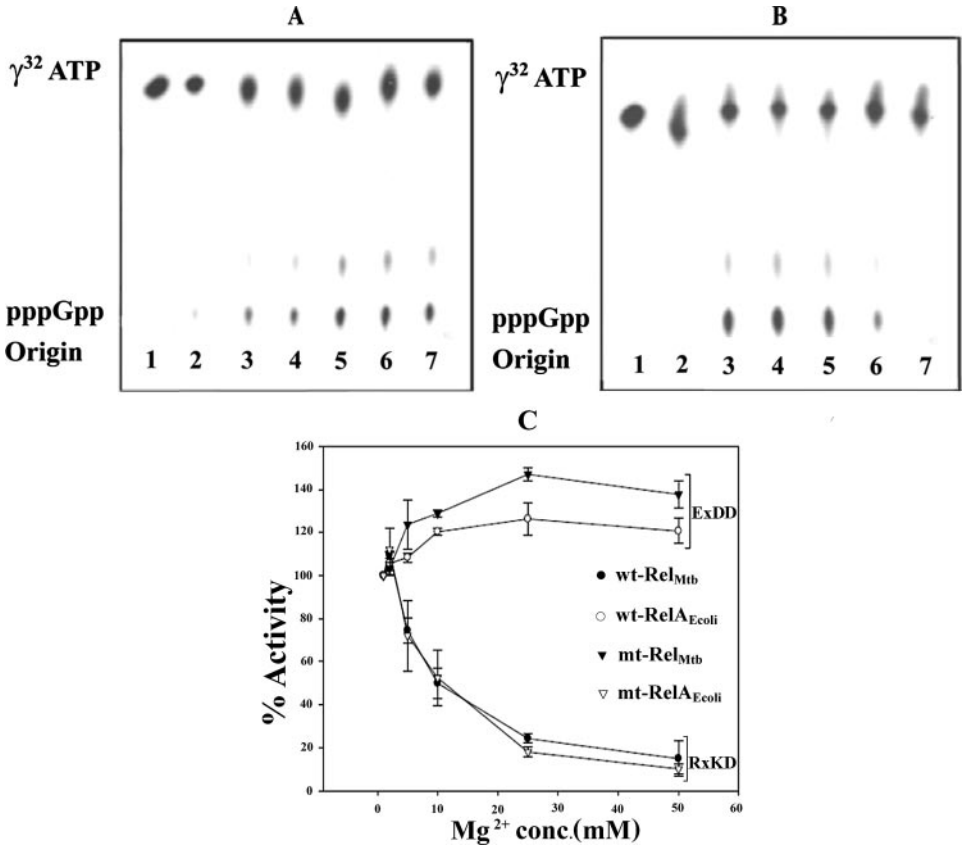

FIGURE 3. **Mutant proteins, with motifs RXKD and EXDD interchanged, show a reversal of Mg^{2+}-dependent inhibition.** pppGpp synthesis assays were carried out on mutants MT-Rel_{Mtb} (*A*) MT-$RelA_{E.\ coli}$ (*B*) under conditions identical to Fig. 1. The amount of pppGpp produced under varying $MgCl_2$ is shown from *lanes 1–7*. *Lane 1*, negative control without the proteins; *lane 2*, 1 mM EDTA (0 mM $MgCl_2$); *lane 3*, 2 mM $MgCl_2$; *lane 4*, 5 mM $MgCl_2$; *lane 5*, 10 mM $MgCl_2$; *lane 6*, 25 mM $MgCl_2$; *lane 7*, 50 mM $MgCl_2$. *C*, quantitation of the results obtained from three independent experiments, similar to those shown in Fig. 1, *A* and *B*, and in *panels A* and *B* of this figure. Spots corresponding to pppGpp were cored out, and the counts were determined. The percentage of activity was calculated with respect to the activity at 1 mM Mg^{2+} that was normalized to 100%. The percentage of pppGpp synthesized by WT-Rel_{Mtb}, MT-Rel_{Mtb}, WT-$RelA_{E.\ coli}$, and MT-$RelA_{E.\ coli}$ are plotted against increasing Mg^{2+} concentration (*Mg^{2+} conc.*).

functional significance of this motif. The absence of bound Mg^{2+} in the structure, despite providing 5 mM $MgCl_2$ during crystallization, indicated that GDP/GTP binding may be Mg^{2+}-independent. The RXKD motif lies in close proximity to the GTP/GDP binding pocket and is well conserved in the bifunctional class. It appeared that this motif could possibly stabilize the β- and γ-phosphates of GTP. In monofunctional proteins, Arg and Lys are substituted by Glu and Asp, respectively, and the EXDD motif is well conserved. We argued that a Mg^{2+} ion coordinated by Glu and Asp provides a similar stabilization to GTP. This led us to hypothesize that, apart from the catalytic Mg^{2+} binding site in these proteins, EXDD forms a second Mg^{2+} binding site in the monofunctional proteins to stabilize GTP and that this charge reversal could explain the differential use of Mg^{2+} by Rel proteins. Further experiments were designed to verify this hypothesis, using mutant proteins that exchanged the RXKD and EXDD motifs in the bifunctional Rel_{Mtb} and monofunctional $RelA_{E.\ coli}$.

Exchanging RXKD and EXDD Motifs Reverses the Effect of Mg^{2+} on pppGpp Synthesis—To verify whether interchanging RXKD and EXDD motifs would reverse the effect of Mg^{2+} on pppGpp synthesis, the conserved arginine (Arg-348) and lysine (Lys-350) residues in the RXKD motif of bifunctional Rel_{Mtb} were mutated to Glu and Asp, respectively. Similarly, Glu-306 and Asp-308 in the EXDD motif of $RelA_{E.\ coli}$ were mutated to Arg and Lys, respectively. (Hereafter, the mutants are referred to with the prefix "MT," and the wild type proteins are referred to with the prefix "WT.") These mutants were purified, and pppGpp synthesis assays were conducted as earlier. In line with our proposal, the mutants reversed the effect of Mg^{2+} on pppGpp synthesis. Fig. 3*A* shows that the amount of pppGpp synthesized by MT-Rel_{Mtb} is not inhibited at high Mg^{2+} when compared with WT-Rel_{Mtb} (Fig. 1*A*). Conversely, Fig. 3*B* shows that pppGpp synthesis by MT-$RelA_{E.\ coli}$ is severely affected, unlike WT-$RelA_{E.\ coli}$ (Fig. 1*B*). These experiments clearly established (Fig. 3*C*) that the motifs RXKD and EXDD play significant roles in determining the differential effect of Mg^{2+} on (p)ppGpp synthesis by Rel proteins. It appears that the inhibitory effect at higher Mg^{2+} is seen for proteins having an RXKD motif and not if they have an EXDD motif (Fig. 3*C*). To further underscore the role of these motifs, fluorescent nucleotide binding and CD experiments were conducted.

RXKD Motif Determines Mg^{2+}-dependent Inhibitory Effect on (p)ppGpp Synthesis—mant-nucleotides are sensitive fluorescent probes to study nucleotide binding in proteins (21). The nucleotide analogues, mant-GTP and mant-ATP, were used to study the significance of RXKD and EXDD motifs in nucleotide binding under varying Mg^{2+} concentrations. Proteins having the RXKD motif, *i.e.* WT-Rel_{Mtb} and MT-$RelA_{E.\ coli}$, bound to mant-GTP and mant-ATP even in the presence of 1 mM EDTA (Fig. 4*A*, *panels 1–4*, colored *blue*), negating the need for Mg^{2+} in nucleotide binding. However, this effect was not obvious for WT-$RelA_{E.\ coli}$ and MT-Rel_{Mtb}, having an EXDD motif (Fig. 4*B*) where no nucleotide binding could be detected. We presume that in these proteins, the nucleotide dissociation constants are very high at equilibrium, and therefore, nucleotide binding in the steady state does not lead to a significant increase in fluorescence.

When the fluorescence experiment was conducted with increasing Mg^{2+}, both GTP and ATP binding to WT-Rel_{Mtb} reduced appreciably (Fig. 4*A*, *panels 1* and *2*). Similarly, MT-$RelA_{E.\ coli}$ (with RXKD) behaved like WT-Rel_{Mtb} (Fig. 4*A*, *panels 3* and *4*) and showed a reduction in nucleotide binding. Interestingly, the exchange of motifs reversed the effect of

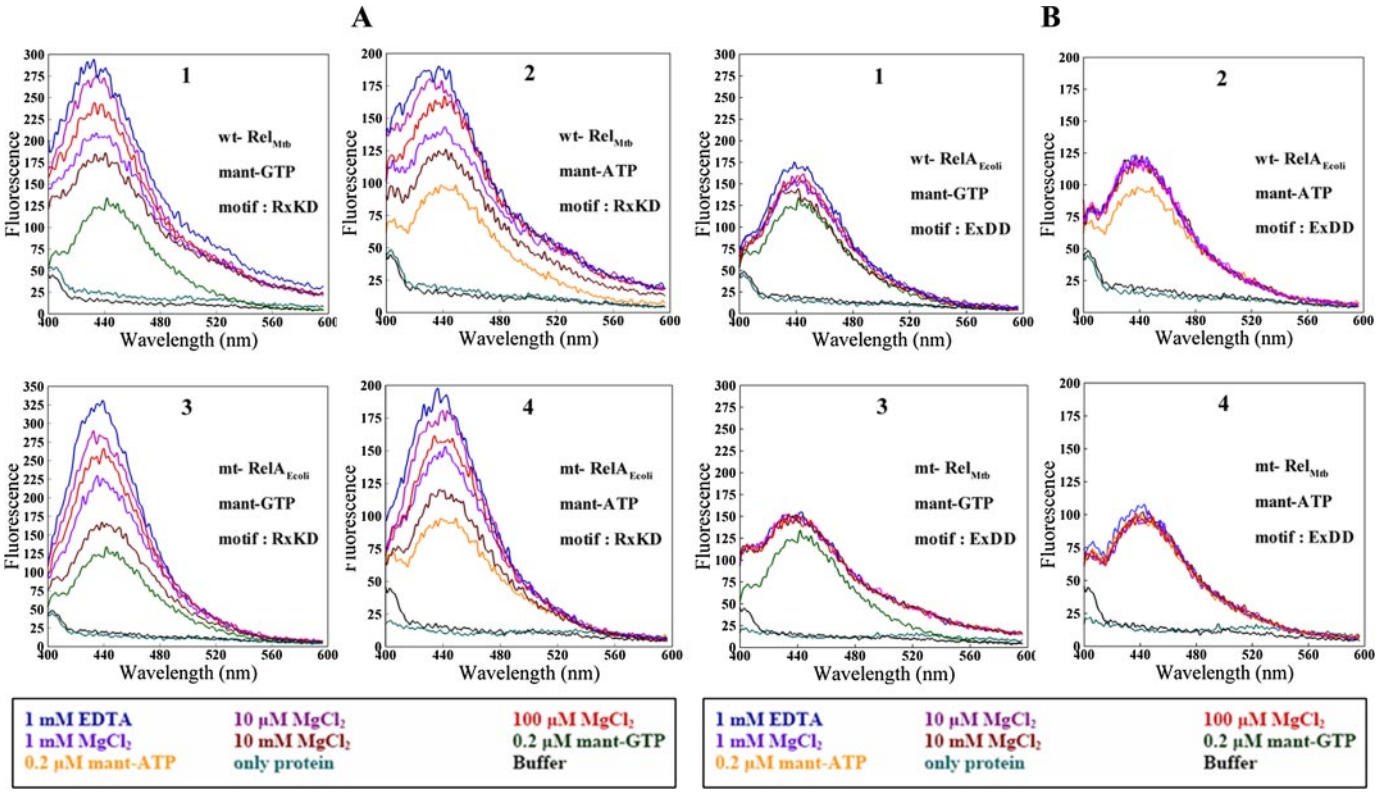

FIGURE 4. **The effect of increasing Mg^{2+} on mant-nucleotide binding to R*X*KD motif-containing proteins (*A*) and E*X*DD motif-containing proteins (*B*).** Shown are emission spectra (λ_{ex} 350 nm) obtained following incubation of 4 μM protein with 0.2 μM mant-nucleotides (ATP/GTP) and in the presence of 1 mM EDTA (*blue*) and varying concentrations of Mg^{2+} as indicated in the *insets*. The proteins and nucleotides used are indicated in the *insets*. Spectra corresponding to various Mg^{2+} concentrations are indicated in different colors.

Mg^{2+} to the extent that MT-Rel$_{Mtb}$ behaved like WT-RelA$_{E.\ coli}$, wherein no nucleotide binding could be detected (Fig. 4*B*). In conclusion, these experiments clearly demonstrate that nucleotide binding is severely affected in the presence of higher Mg^{2+} when the proteins carry an R*X*KD motif (*i.e.* WT-Rel$_{Mtb}$ and MT-RelA $_{E.\ coli}$). This is in line with the effect seen on pppGpp synthesis (Figs. 1 and 3).

Mg^{2+} Induces a Structural Transition in RXKD-containing Rel Proteins—Based on the structure of Rel$_{Seq}$, an interesting feature suggested by Hogg *et al.* (20) is a structural transition of a loop (α13/β4 loop), termed "catalytic loop," situated in the synthesis domain. This loop was postulated to be involved in Mg^{2+}-ATP binding. As fluorescence studies revealed that Mg^{2+} affects nucleotide binding (Fig. 4), we wanted to test whether Mg^{2+} alone could influence any structural transitions in the protein. Thus, all CD experiments were carried out in the absence of nucleotides and with varying Mg^{2+} concentrations. We observed an increase in helical content for WT-Rel$_{Mtb}$ with increasing concentration of Mg^{2+} (Fig. 5*A*). However, under similar conditions, there was no significant difference in the helical content of WT-RelA$_{E.\ coli}$ (Fig. 5*D*). Interestingly, like the reversals in pppGpp synthesis and nucleotide binding, the structural transition (*i.e.* increase in helical content) was also reversed in MT-Rel$_{Mtb}$ having an E*X*DD motif (Fig. 5*B*). In MT-RelA$_{E.\ coli}$ where E*X*DD is replaced with R*X*KD, this reversal is not apparent at lower concentration of Mg^{2+} (up to 5 mM) but is clearly noticed at 10 mM Mg^{2+} (Fig. 5*C*). It is possible that an increase in helicity would be observed at higher concentrations if experimental limitations did not restrict us to minimal Mg^{2+} concentrations (22, 23). Overall, the data from the CD experiments suggest that an increase in helical content in Rel proteins occurs only when they carry an R*X*KD motif and also that this effect is solely due to Mg^{2+} as ATP and GTP were not supplied in these experiments. Hence, together with the nucleotide binding studies, it is tempting to speculate that the increase in helical content is possibly associated with the loop-to-helix transition of the catalytic loop proposed by Hogg *et al.* (20).

DISCUSSION

The metabolism of (p)ppGpp is dependent on metal ions where Mg^{2+} is utilized for the synthesis reaction that involves a pyrophosphate transfer from ATP to GTP/GDP/IMP. Rel proteins are classified along with enzymes such as DNA Polβ that catalyze a similar reaction. Most biochemical studies, supported by crystal structures, suggest a dual metal ion mechanism for DNA Polβ (19, 25, 26). Three conserved Asp residues at the active site are proposed to coordinate the binding of two Mg^{2+} ions and ATP at the active site. There is little effect on the polymerase activity of DNA Polβ as Mg^{2+} is increased (27). However, reports by Avarbock *et al.* (17) and Mechold *et al.* (18) suggest that a similar mechanism may not prevail in Rel$_{Mtb}$ and Rel$_{Seq}$ as they observe a severe inhibition of pppGpp synthesis at high Mg^{2+} concentration. Based on these and the lack of a third conserved Asp in the structural comparison of Rel$_{Seq}$ and Polβ,

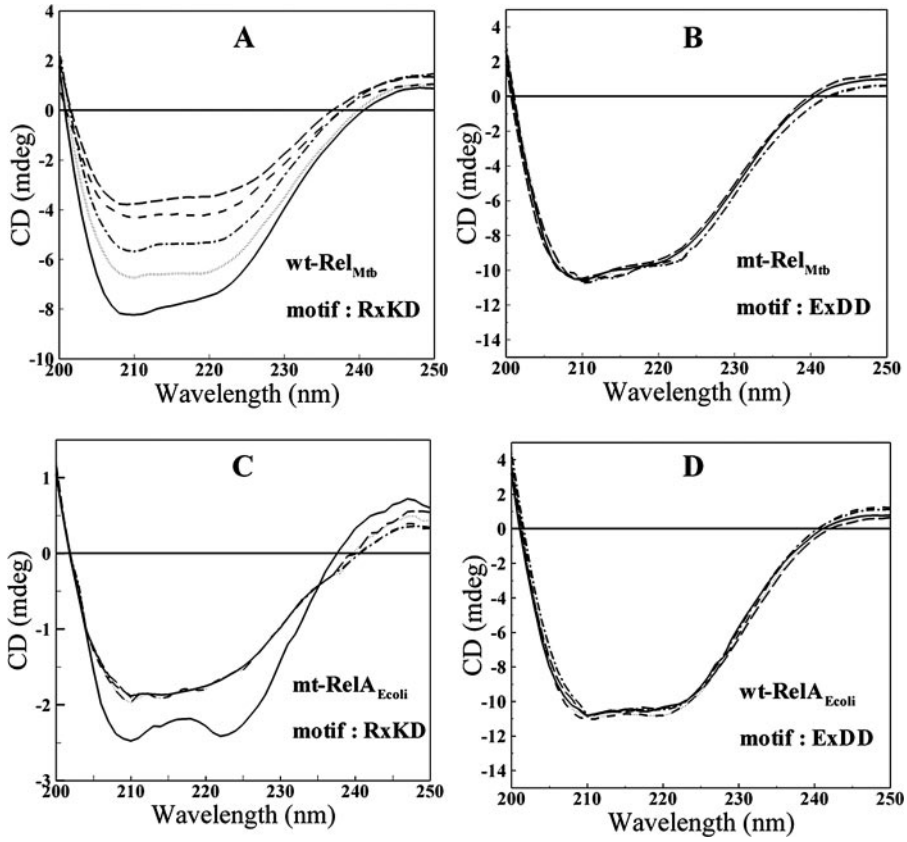

FIGURE 5. **Increasing Mg^{2+} induces an increase in helical content in Rel proteins carrying an R*X*KD motif.** Circular dichroism spectra were recorded as follows. *A*, WT-Rel$_{Mtb}$; *B*, MT-Rel$_{Mtb}$; *C*, MT-RelA$_{E.\ coli}$; *D*, WT-RelA$_{E.\ coli}$. in the absence of nucleotides, but with increasing Mg^{2+}. The experiment was conducted with 0 mM $MgCl_2$ (– – –), 10 μM $MgCl_2$ (——), 100 μM $MgCl_2$ (·–·–·–), 1 mM $MgCl_2$ (····), and 10 mM $MgCl_2$ (——). *mdeg*, millidegrees.

Hogg *et al.* (20) proposed a single-cation mechanism for Rel proteins.

Here, we distinguish between the bifunctional and monofunctional classes of Rel proteins and show that they utilize Mg^{2+} differentially for the (p)ppGpp synthesis activity. We associate this difference in metal requirement to a unique charge reversal in a conserved motif of the synthesizing domain. The significance of this charge reversal is revealed in pppGpp synthesis assays using the wild type and mutant Rel$_{Mtb}$ and Rel$_{E.\ coli}$ (Fig. 3*C*), which clearly suggests that the presence of R*X*KD/E*X*DD motif determines this differential effect. The inhibition due to Mg^{2+} is restricted only to proteins containing an R*X*KD motif.

Furthermore, fluorescence studies revealed the influence of R*X*KD/E*X*DD motifs in determining nucleotide binding in the presence of Mg^{2+}. Firstly, both GTP and ATP binding are Mg^{2+}-independent for proteins having an R*X*KD motif since WT-Rel$_{Mtb}$ and MT-RelA$_{E.\ coli}$ bind nucleotides even in Mg^{2+}-depleted (with EDTA) conditions (Fig. 4*A*, colored *blue*). Secondly, GTP and ATP binding reduced considerably in WT-Rel$_{Mtb}$ that carried an R*X*KD motif as Mg^{2+} concentration was increased (Fig. 4*A*, *panels 1* and *2*). Although this effect was not seen for RelA$_{E.\ coli}$ (with E*X*DD), MT-RelA$_{E.\ coli}$ carrying an R*X*KD motif showed a clear reversal as nucleotide binding reduced at higher Mg^{2+} (Fig. 4*A*, *panels 3* and *4*). Thus, it is apparent that R*X*KD-containing proteins do not bind nucleotides at high Mg^{2+} and therefore explains the lack of pppGpp synthesis seen in Figs. 1*A* and 3*B*.

Our observation from CD experiments, that R*X*KD-containing proteins show an increase in helicity (Fig. 5, *A* and *C*) with increasing Mg^{2+}, gains prominence due to the fact that a similar loop-to-helix transition of a region, termed catalytic loop, is implicated in Mg^{2+} binding in the bifunctional Rel$_{Seq}$ (20). In Rel$_{Seq}$, two monomers present in the asymmetric unit display a conformational antagonism, *i.e.* in one monomer, the synthesis domain is inactive and the hydrolysis domain is active (synthesis-OFF/hydrolysis-ON) and *vice versa* in the second monomer (synthesis-ON/hydrolysis-OFF). The catalytic loop is unstructured when the synthesis domain is inactive and forms a helical structure when the synthesis domain is active. The importance of this structural transition arises due to the way Mg^{2+} is proposed to be coordinated. Two conserved residues, Asp-264 of the catalytic loop and Glu-323 from a neighboring β-sheet, coordinate the Mg^{2+}. As this β-sheet is a part of the rigid core that confers stability to the domain, we assume that Mg^{2+} binding is determined by an appropriately positioned Asp-264 (and Glu-323). This positioning of Asp-264 could be achieved by the structural transition of the catalytic loop to a helix, and hence, could regulate Mg^{2+} binding. Hogg *et al.* (20) proposed that the catalytic loop undergoes this transition when Mg^{2+} binds together with ATP. However, for proteins having an R*X*KD motif, fluorescent nucleotide binding experiments clearly depict that ATP binding is Mg^{2+} independent (Fig. 4*A*, colored *blue*), and the CD experiments reveal that the structural transition, too, is exclusively due to Mg^{2+} (Fig. 5, *A* and *C*). Altogether, it is likely that the structural transition noticed in the CD experiments is largely of the catalytic loop observed in the structure of Rel$_{Seq}$ (20).

The differential effect of Mg^{2+} on pppGpp synthesis, nucleotide binding, and CD experiments can be rationalized as follows. In the case of R*X*KD-containing bifunctional proteins, perhaps the loop-to-helix transition of the catalytic loop induced by Mg^{2+} leads to a closure of the substrate binding pocket such that ATP and GTP are excluded from it, which leads to the lack of (p)ppGpp synthesis. In the case of E*X*DD-containing proteins, Mg^{2+} is unable to induce a similar structural change, and hence, does not affect (p)ppGpp synthesis. This may be due to a second Mg^{2+} binding site coordinated by Glu and Asp of E*X*DD in the monofunctional proteins, where GTP could be stabilized by this additional Mg^{2+} ion (see

"Results"). Perhaps Mg^{2+} binding to the second site prevents the structural transition of the catalytic loop at high Mg^{2+}. This difference suggests that unlike bifunctional Rel proteins that follow a single-metal ion-mediated catalysis, monofunctional proteins use an additional metal ion for (p)ppGpp synthesis. However, the second metal ion is dispensable since the mutation of E*X*DD to R*X*KD retains synthesis activity in monofunctional $RelA_{E.\ coli}$.

Acknowledgments—We thank A. Ravi Kant for help with preparing Figs. 4 and 5 and P. Baral for initial efforts on Rel projects. Our sincere thanks also go to Drs. R. Gokhale, R. P. Roy, R. Gurunath, and J. Bera for the use of fluorescence and CD facilities and for useful discussions. We also thank N. S. Yadav and D. Joshi for excellent secretarial and technical assistance.

REFERENCES

1. Braeken, K., Moris, M., Daniels, R., Vanderleyden, J., and Michiels, J. (2006) *Trends Microbiol.* **14,** 45–54
2. Magnusson, L. U., Farewell, A., and Nystrom, T. (2005) *Trends Microbiol.* **13,** 236–242
3. Cashel, M., Gentry, D. R., Hernandez, V. J., and Vinella, D. (1996) *Escherichia coli and Salmonella: Cellular and Molecular Biology* (Neidhardt, F. C.), Vol. 2, pp. 1458–1496, American Society for Microbiology, Washington, D. C.
4. Gralla, J. D. (2005) *Mol. Microbiol.* **55,** 973–977
5. Wagner, R. (2002) *J. Mol. Microbiol. Biotechnol.* **4,** 331–340
6. Artsimovitch, I., Patlan, V., Sekine, S., Vassylyeva, M. N., Hosaka, T., Ochi, K., Yokoyama, S., and Vassylyev, D. G. (2004) *Cell* **117,** 299–310
7. Primm, T. P., Anderson, S. J., Mizrahi, V., Avarbock, D., Rubin, H., and Berry, C. E., III (2000) *J. Bacteriol.* **192,** 4889–4898
8. Dahl, J. L., Krus, C. N., Boshoff, H. I. M., Doan, B., Foley, K., Avarbock, D., Kaplan, G., Mizrahi, V., Rubin, H., and Barry, C. E. (2003) *Proc. Natl. Acad. Sci. U. S. A.* **100,** 10026–10031
9. van Delden, C., Comte, R., and Bally, A. M. (2001) *J. Bacteriol.* **193,** 5376–5384
10. Sun, J., Hesketh, A., and Bibb, M. (2001) *J. Bacteriol.* **193,** 3488–3498
11. Kuhar, I., van Putten, J. P., Zgur-Bertok, D., Gaastra, W., and Jordi, B. J. (2001) *Mol. Microbiol.* **41,** 207–216
12. Hammer, B. K., Tateda, E. S., and Swanson, M. S. (2002) *Mol. Microbiol.* **44,** 107–119
13. van der Biezen, E. A., Sun, J., Coleman, M. J., Bibb, M. J., and Jones, J. D. G. (2000) *Proc. Natl. Acad. Sci. U. S. A.* **97,** 3747–3752
14. Jain, V., Saleem-Batcha, R., and Chatterji, D. (2007) *Biophys. Chem.* **127,** 41–50
15. Avarbock, A., Avarbock, D. J. S., Buckstein, M., Wang, Z. M., and Rubin, H. (2005) *Biochemistry* **44,** 9913–9923
16. Aravind, L., and Koonin, E. V. (1998) *Trends Biochem. Sci.* **23,** 469–472
17. Avarbock, D., Avarbock, A., and Rubin, H. (2000) *Biochemistry* **39,** 11640–11648
18. Mechold, U., Murphy, H., Brown, L., and Cashel, M. (2002) *J. Bacteriol.* **194,** 2878–2888
19. Sawaya, M. R., Prasad, R., Wilson, S. H., Kraut, J., and Pelletier, H. (1997) *Biochemistry* **36,** 11205–11215
20. Hogg, T., Mechold, U., Malke, H., Cashel, M., and Hilgenfeld, R. (2004) *Cell* **117,** 57–68
21. Remmers, A. E., Posner, R., and Neubig, R. R. (1994) *J. Biol. Chem.* **269,** 13771–13778
22. Kelly, S. M., Jess, T. J., and Price, N. C. (2005) *Biochim. Biophys. Acta* **1751,** 119–139
23. Kelly, S. M., and Price, N. C. (2000) *Curr. Protein Pept. Sci.* **1,** 349–384
24. Thompson, J. D., Gibson, T. J., Plewniak, F., Jeanmougin, F., and Higgins, D. G. (1997) *Nucleic Acids Res.* **24,** 4876–4882
25. Steitz, T. A. (1998) *Nature* **391,** 231–232
26. Doublié, S., Tabor, S., Long, A. M., Richardson, C. C., and Ellenberger, T. (1998) *Nature* **391,** 251–258
27. Black, C. B., and Cowan, J. A. (1998) *J. Biol. Inorg. Chem.* **3,** 292–299

A Charge Reversal Differentiates (p)ppGpp Synthesis by Monofunctional and Bifunctional Rel Proteins

Mathew Sajish, Divya Tiwari, Dimple Rananaware, Vinay Kumar Nandicoori and Balaji Prakash

J. Biol. Chem. 2007, 282:34977-34983.
doi: 10.1074/jbc.M704828200 originally published online October 2, 2007
